

## **COMPUTATIONAL MOLECULAR NANOSTRUCTURES AND MECHANICAL/ADHESION PROPERTIES OF HYDROXYAPATITE**

V. Bystrov, E. Paramonova, N. Bystrova, A. Saprionova, S. Filippov

*Institute of Mathematical Problems of Biology RAS, Pushchino, 142290,  
Moscow region, Russia, e-mail: bystrov@impb.psn.ru, vsbys@yahoo.co.uk*

### **ABSTRACT**

The present work is focused on computational physics investigation and computer simulation for hydroxyapatite (HAP) nanostructures, explore the possible mechanisms on its surface charging, based on proton transfer, and discussion of the adhesion/cohesion properties of HAP nanoparticles. It is focused on computational physics investigation and computer simulation for hydroxyapatite (HAP) nanostructures, explore the possible mechanisms on its surface charging, based on proton transfer, and discussion of the adhesion/cohesion properties of HAP nanoparticles. Computer models (including 3-D animation) of HAP nanostructures are constructed on the basis of quantum-chemical and soliton approaches for various groups of symmetry with the help of adaptation of programs HyperChem, Crystal, Gaussian-98 and with some own additionally elaborated software. Structural peculiarities of HAP nanoparticles (such as formation of proton channels along c-axis) are established, that clears up the mechanism of the surface's charging for HAP-

nanoparticles - the proton mechanism of polarization is proposed. The values of surface charges density is estimated about  $0,1 \text{ C/m}^2$ , creating electric field up  $10^5 \dots 10^7 \text{ V/m}$  in the media and influencing on the living cells motion and adhesion (immobilization) on the HAP surface.

## 1. INTRODUCTION

**Hydroxyapatite [ $\text{Ca}_5(\text{PO}_4)_3\text{OH}$ ; (HAP)] structures** have been wide used over past time in medicine as an innate bioactive ceramics materials for bones and dentals implants, because their crystal structure and composition are very analogous with the hard tissues of living bone, corresponds to structure of a mineral bone's component, that leads to the new bone formation generated by osteoblasts growth on its surface [1-3]. Recently investigations demonstrated that polarized HAP has some specific surface characteristics and provide the additional stimulation of the interaction with living cells [3]. The HAP adhesion properties were improved, if the HAP surface was charged. The mechanisms of polarization and changes of surface electrical, mechanical and adhesive properties are not yet clear. The arising of the polarization is caused by processes of charge (proton) transfers by the HAP nanostructural components. These processes have electrets-like character, because are influenced by electric field and temperature, as was discussed in [4], but haven't ferroelectric-like type [5 – 8].

In the present work we try to understand the HAP structural changes by using the computer simulation of HAP crystal nanostructures. For these purposes in the given work the computer models are considered and the mechanisms of charge transfer are analyzed on the base of known HAP structural data [9] using the HyperChem and Crystals software [10]. Additionally now we try to use the Gaussian 98 [11] code for development of further HAP structural optimization.

This work is connected with the FP6 EC project NMP3-CT-2003-504937 “PERCERAMICS” and will develop a percolated nanostructured electrically polarized ceramics fabricated from HAP to improve quality of bone eligible bioimplants, work out new material for immobilization of microorganisms for their further use to product of various biologically active compounds and purify the environment. A surface of this HAP electrically charged ceramics would provide a relevant biological – non-biological interface to adhere cells or microorganisms.

A surface morphology of such HAP polarized ceramics will be supplied at a nano scale eligible for a cell receptor “tail” size and will be “packed” from HAP nanoparticles. For this purpose the HAP ceramics surface will be charged and supplied with a web of the canals. The present work is first step of computational physics investigation and computer modelling for HAP nanostructure, explore the possible mechanisms on its surface charging and adhesion/cohesion properties of HAP nanoparticles.

## **2. INFLUENCE OF HAP SURFACE CHARGES ON PHYSICAL PROPERTIES AND CELL ADHESION**

Influence of HAP surface state, its electrical, mechanical and adhesive properties, particularly, value and polarity of surface charges on the adhesion/cohesion properties and activity of living cells, is very important and actual for different biomedical and biotechnological applications. As it is known the surface charge  $Q$  of a material has significant effect on the adhesion and crystallization [1, 12-14] of inorganic ions and biopolymeric compounds dissolved in aqueous or non-aqueous solutions. The dielectric material used to be the sources of electrostatic charges are materials, which retain long lasting polarization, such as electrets and ferroelectrics [5-8, 12]. It may be as polymers as crystals or ceramics structure. One of the wide used now in

biology and medicine surface-charged ceramics is hydroxyapatite (HAP) [1-3, 13-17], the most stable with respect to dehydration [ 4, 18, 19].

Surface charges of biomaterials are recognized as one of the important factors in determining biologic responses. The effect of the surface charges are directly propagated to cells as well as indirectly via ionic and macromolecular substances adsorbed onto the materials. Hench et al. [20] proposed as a bone-bonding mechanism of bioactive ceramics, an electrostatic chemical bond between the negative-charged oxygen of the material surfaces and the amine groups of the amino acids. Krukowski et al. [21] showed that negatively charged polymer beads promote bone formation at 1 month after implantation in rats while the vicinity of positively charged beads a dense connective tissue is formed. On the contrary, their former report described that the positively charged surfaces of the polymers were accompanied by new bone formation at 1 week after implantation in chicken femora, whereas negatively charged and uncharged beads were non-osteoconductive [22].

The biological effects of HAP is well known, especially affected the polarized surface-charged HAP. In particular, these materials have prominent effects on proliferation of microorganisms, such as osteoblastic cells [13], gram-positive and –negative bacteria [23], and have reconstructive interaction with bone tissue [14]. Although the effects of the charges on HAP surface still are controversial, both negative and positive charges influenced on biological cells activities on its surfaces. For example, from last experimental data of Nakamura et al. [3], follows, that the charged surfaces of electrically polarized HAP ceramics were demonstrated to enhance osteoconductivity significantly cooperated with the innate bioactivity of HAP and promoted the bone reconstruction in the wide defects more then did the nonpolarized HAP ceramic surface, but the processes varied according to the charge polarity.

Extensively large surface charges (more then  $0,15 \text{ C/m}^2$  according to last published data by Nakamura et al. [4]) are inducible on HAP ceramics by

proton transport polarization as were proposed by various authors [1-4, 15,16,18].

Now, we shortly considered the peculiarities of HAP structure and possible discussed mechanisms of these effects of HAP polarization.

### 3. HAP STRUCTURE AND MECHANISMS OF CHARGES TRANSFER AND POLARIZATION OF HAP

Main physical properties of HAP crystal structure, such as ion conductivity and polarization, are explained by nanostructural peculiarities of HAP as existence of the channels parallel with  $c$  axes. This channel in HAP consists of one-dimensional  $\text{OH}^-$  - chains (see simple model of this cases on Fig.1. a, b). The protons occupy the top and bottom party  $\text{O}_2^-$  by a casual image with equal probability in hexagonal HAP structure.

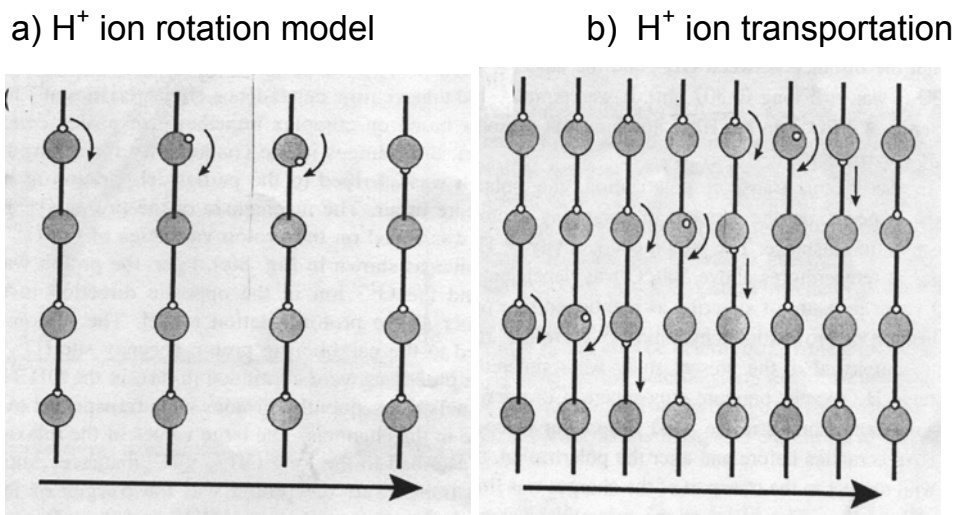


Figure 1: Model of one-dimensional  $\text{OH}^-$ -chains and proton motions (from [3]).

On the contrary, in the monoclinic phase the direction of a proton in all channels which are taking place in the same plane, parallel plane  $a, c$ , is identical: either all upwards, or all downwards. The next plane  $b/2$  is always

focused in the opposite party. The ions  $\text{OH}^-$  are surrounded with two pairs next  $\text{Ca}_2^+$  triangles in both structures: both in hexagonal, and in monoclinic [1,2]. The following mechanisms of a charge transfer are wide discussed in literature [1-4]. As more probable: polarization and depolarization are attributed to rotation of a proton around  $\text{OH}^-$  in colon-like channels, and the mechanism of proton conductivity based on proton vacancies  $\text{O}_2^-$  in ions  $\text{OH}^-$ , where as well as in model of proton rotation, proton turns around of an ion  $\text{O}_2^-$  in opposite an initial direction. Then the proton moves to the next proton vacancy  $\text{O}_2^-$ . When such process proceeds further on  $\text{OH}^-$  to the channels, there is a proton transfer on the large distances in the channels. The large relaxation times are attributed to the large distance of the  $\text{OH}^- - \text{OH}^-$  ( $\sim 0,344$  nm). The polarizing charge under the polarization process by means of the proton transport depends on the number of migrated protons and extent of migration [3]. It is very important that both these parameters are controlled by the temperature and electric field.

Another model is connected with the main role of dipoles reorientation [2, 15]. As it is mentioned above and is known, HAP can occur in a monoclinic phase (space group  $P2_1/b$ ) or in the hexagonal system ( $P6_3/m$ ) according to the temperature and how nearly stoichiometric they are. In this case the authors [2, 15] usually were particularly interested here in dipole reorientations similar to those in the monoclinic-hexagonal phase transition observed in some HAP. Which phase is present depends directly on the ordering of the dipoles in the “tunnels”, i.e. in the tunnel-shaped regions occupied by linear  $\text{OH}^-$  channels in the HAP structure. In the monoclinic phase, all of the dipoles in all of the tunnels lying in the same plane parallel to the  $a,c$  plane must be either all up or all down and those in the next plane  $b/2$  away must be oriented oppositely. When there is a sufficient departure from stoichiometry, or when growth conditions did not provide enough ion mobility so that the minimum free-energy configuration was attained, consecutive chains of  $\text{OH}^-$  dipoles in the same tunnel may be oriented differently (“disordered column” model of

hexagonal phase) or they may be oriented in the same way inside the given tunnel, but that orientation is independent from the orientation in neighboring tunnels (ordered column model of the hexagonal phase). The hexagonal phase is then statically stabilized at room temperature. When the temperature is sufficiently elevated, e.g. near 200 °C, chains of OH<sup>-</sup> dipoles are able to reverse their orientations and thus to produce the hexagonal phase, if it was not already present. The hexagonal phase is then quasi-statically stabilized. At a still higher temperature, e.g. 350-450 °C, the OH<sup>-</sup> ions acquire enough thermal energy to reorient “at will” independently of their OH<sup>-</sup> neighbors in the chain. The hexagonal phase is then dynamically stabilized. The monoclinic-hexagonal transition: temperature  $T_{c1} = T_{c2} = 211.5$  °C and relaxation times  $T_{c1} = 7.0 \times 10^{-4}$  s and  $T_{c2} = 7.7 \times 10^{-4}$  s. At this temperature, the hexagonal phase is quasi-statically stabilized against the monoclinic. But, as it is clear, from this consideration that this model approach connect with proton switching and transfer on the OH-chains, too. Therefore, in any case, we have the same proton motion along H-OH chains and we can to use some generalized description of this proton motions.

#### **4. PROPOSED MODEL AND COMPUTER MODELING OF HAP STRUCTURE APPROACHES, RESULTS AND DISCUSSION**

We consider the model of HAP nanostructure and polarization mechanism based on the model of proton transfer and “switching” along OH-like chains, its transport and migration under influence of external electric field. This approach was developed for the case of proton transport and switching in our recent papers [24 -26]. To explore these processes by quantum-chemical methods (using the calculations of Potential Energy Surface – PES – for determination of probability of proton transfer) in HAP it is necessary firstly to construct the ab initio quantum-chemical model of HAP nanostructure.

For this first stage of the HAP structure determination, transformation, proton charges transfer and HAP surface polarization we explore the initial HAP structure in this work. We're used data on HAP structure from [9], presented in the following table 1.

Table 1: The experimental crystallographic data of relative coordinates x, y and z of HAP elementary cell structure from [9]. (Additional data - abbreviations Biso, B(x,x) – presented in this table are explained more detailed in the same site [9]).

atom	x	y	z	B iso	B (1,1)	B (2,2)	B (3,3)	B (1,2)	B (1,3)
Ca1	0.66667	0.33333	0.00144		0.00408	0.00408	0.0033	0.00204	0
Ca2	-0.00657	0.24706	0.25		0.00308	0.00353	0.00417	0.00156	0
P	0.36860	0.39866	0.25		0.00223	0.0025	0.0034	0.00127	0
O 1	0.48500	0.32890	0.25		0.0036	0.0044	0.0059	0.0027	0
O 2	0.46490	0.58710	0.25		0.0035	0.0031	0.0105	0.0016	0
O 3	0.25800	0.34350	0.0703		0.005	0.0096	0.007	0.00505	-0.0025
O (H)	0	0	0.1979		0.003	0.003	0.012	0.0015	0
H	0	0	0.04	3.3					

As the entrance data (initial file) for Crystals software the relative coordinates x, y, z from the above given table 1 multiplied by the appropriate parameters of a cell were used.

For our calculations and computer modelling we use these data with account that absolute values of HAP crystal elementary cell unit parameters are:  $a = b = 9.42$  Angstrom = 0.942 nm,  $c = 6.87$  Angstrom = 0.687 nm.

Parameters of a cell and group of symmetry of a crystal also were set: P6/m and P6<sub>3</sub>/m.

In the program Crystals [9] are received the \*.pdb file with coordinates of all atoms (for one and several channels) and qualitative images of HAP structure. Several of the obtained results are presented in Fig. 2. But these visual results obtained from Crystals software are not suitable for good visual atomic representation.

After series of transformation of models representation by special computer software, we obtain HAP nanostructures in several different modes with more suitable visual atomic representation for the same analyzed both symmetry groups  $P 6/m$  and  $P 6_3/m$ , presented on Fig. 3 – 6. For this purpose, the three-dimensional computer model of a crystal was constructed from an output \*.pdb file of Crystals program about the help of additional software “plug-in” Voxel (which was specially elaborated and developed in the IMPB) for Maxon Cinema 4D 8.5. In some cases we construct the atomic visual images with use the HyperChem software, e.g. for more detailed construction of H-OH-... chains image inside the channel for the case of only the one channel presentation (see Figs. 4 (a), (b) below.)

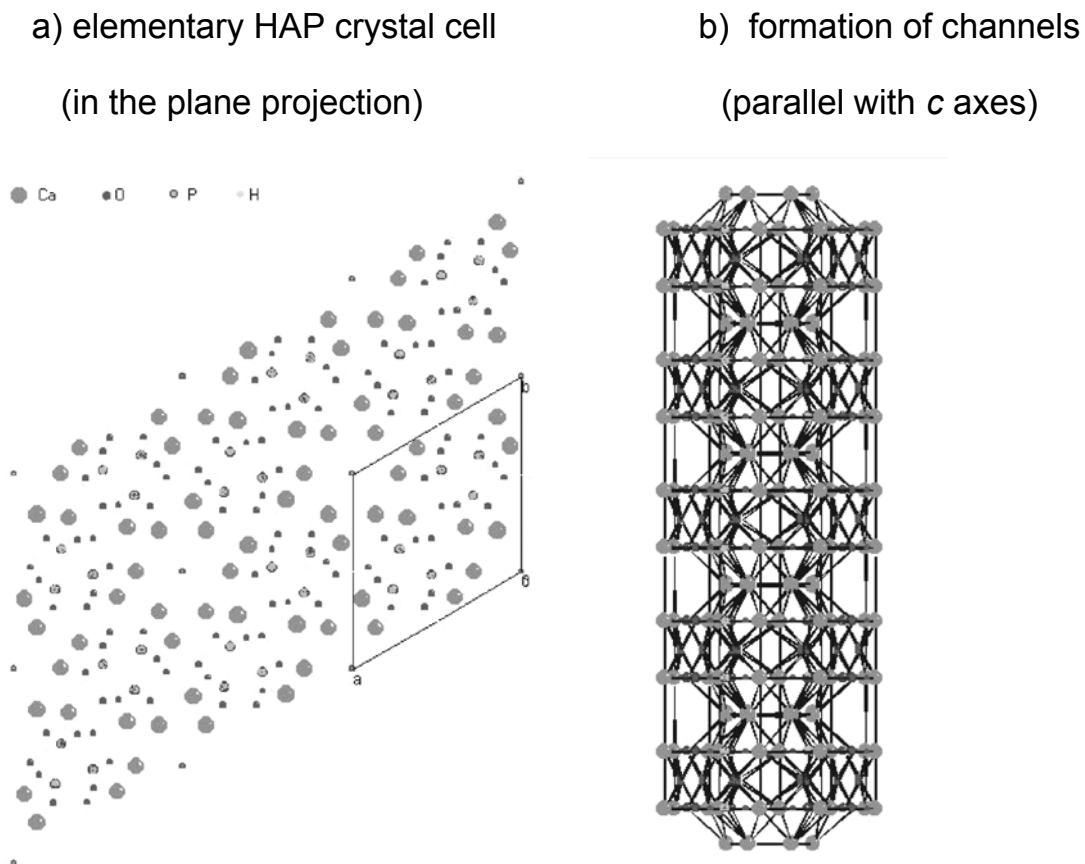
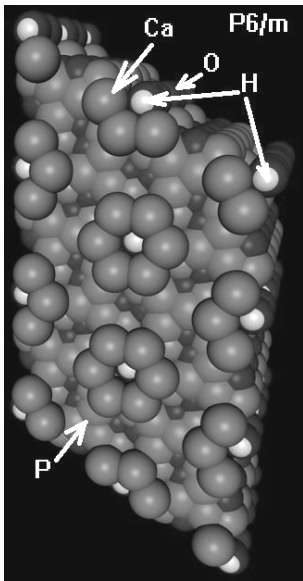


Figure 2: The -by HyperChem and Crystal programs- calculated HAP nanostructure ( $P 6/m$ ).

We obtain firstly the computer model of HAP nanostructure in the hexagonal phase system ( $P6\ 3/m$  symmetry) for several crystal cells. The size of simulated HAP nanoparticles is in the order  $\sim 40\dots60$  Angstrom  $\sim 4\dots6$  nm, and in some case up 100 Angstrom  $\sim 10$  nm, as follows from its cell's parameters and are showed on Figs 2 - 6.

a) view on the HAP surface



b) video-fragment of HAP animation

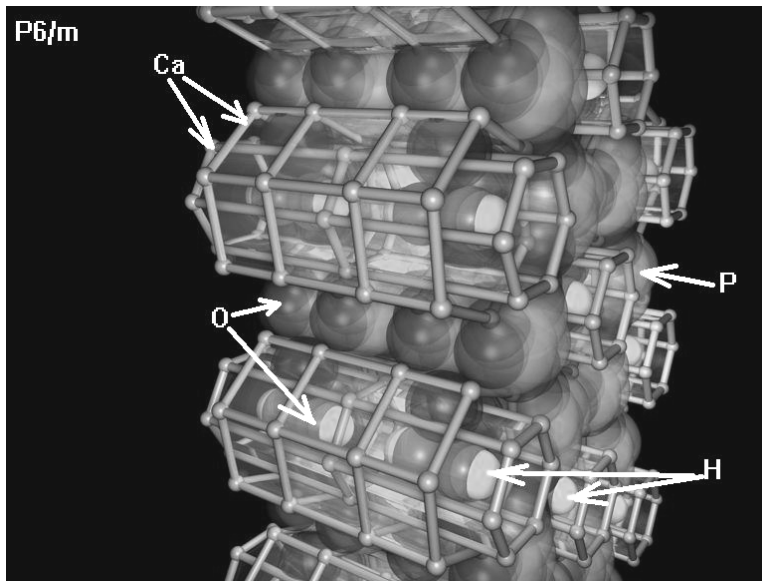


Figure 3: Explored initial three-dimensional HAP structure and video-fragment (group of symmetry are:  $P6/m$ ).

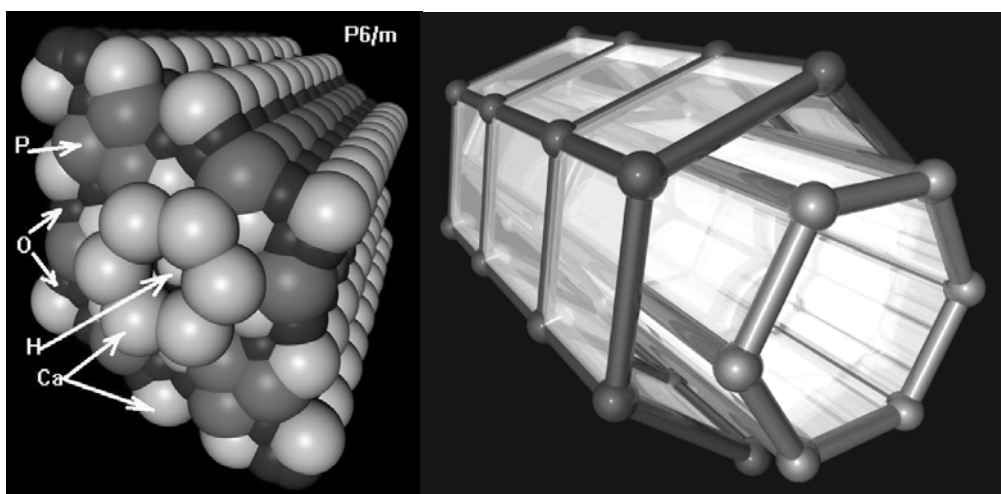


Figure 4: (a, b). Three-dimensional HAP structures (cases are the same as above Figs, but present the HAP nanostructures with only one channel for more detailed images of H-OH... chains inside the channel, that explain further our

model of proton transport along this channel and formation of polarized (charged) surface of HAP nanoparticles),  $P 6/m$  symmetry.

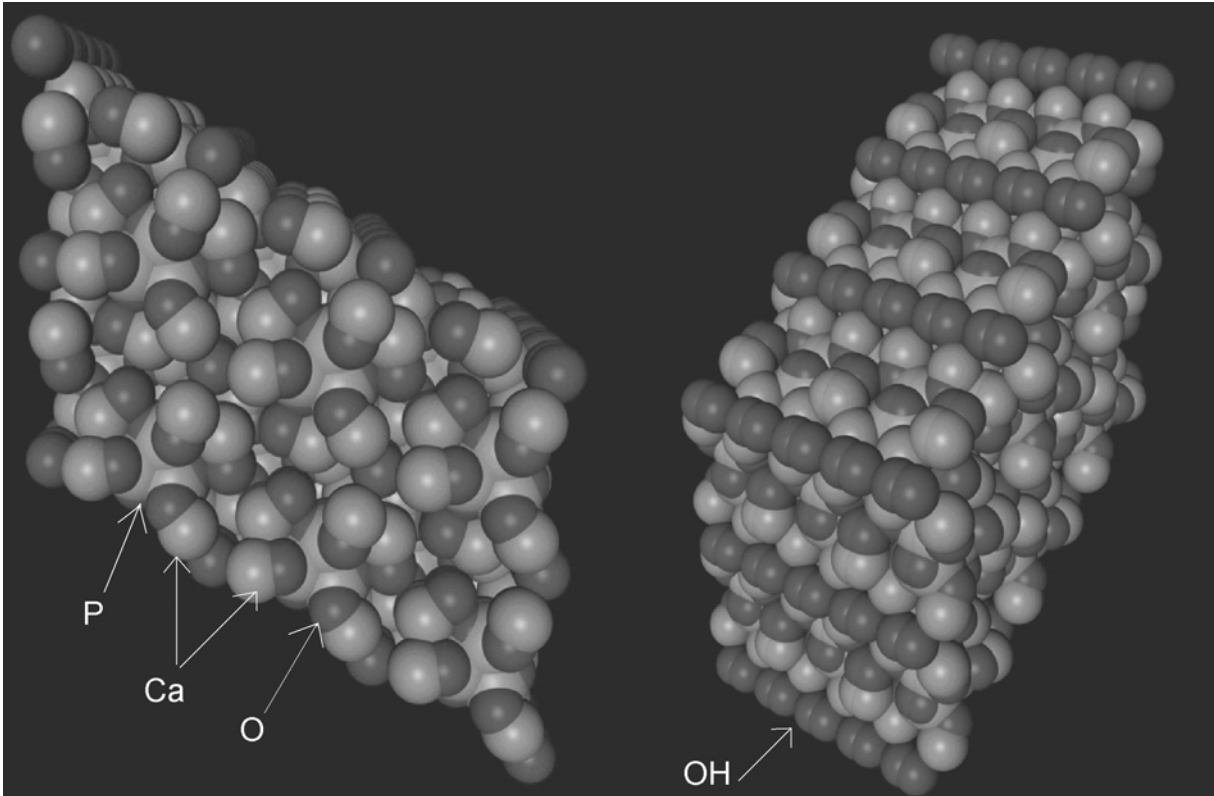


Figure 5: Explored initial three-dimensional HAP structure (group of symmetry is:  $P6_3/m$ ).

The atomic abbreviations are the same as above (it is show on the Figs 3., 4., too). The presentation of HAP surface and three-dimension structure of HAP nanoparticles have another images in this case, that lead the some another channels formation and another physical properties.

The estimated value of surface charge density (for hexagonal  $P 6/m$  group of symmetry) is  $\sim 0,1 \text{ C/m}^2$ , as follows from data of cell parameters ( $a = b = 0,94 \text{ nm} \sim 1 \text{ nm}$ ) and proposal that we have 1 proton excess on the one crystal cell unit (if only one proton migrate from one crystal cell unit on the surface of modeling HAP nanoparticles).

The next step of our exploration was to create the animation computer model of this HAP nanostructure and nanoparticle to show directly the details of OH-

channel for proton transfer and to visualize the proton motion along this channel.

The constructed three-dimensional computer HAP model images for different space projections (obtained by above described special elaborated software addition for Maxon Cinema 4D 8.5) were composed together into computer video fragments.

The resulted videofragments are received in the “discreet combustion 3”. Some examples of these results are presented on Fig. 3 (b) as one three-dimension image. The total files of HAP nanostructure animation, now are presented and available on the web-site of our institute [27].

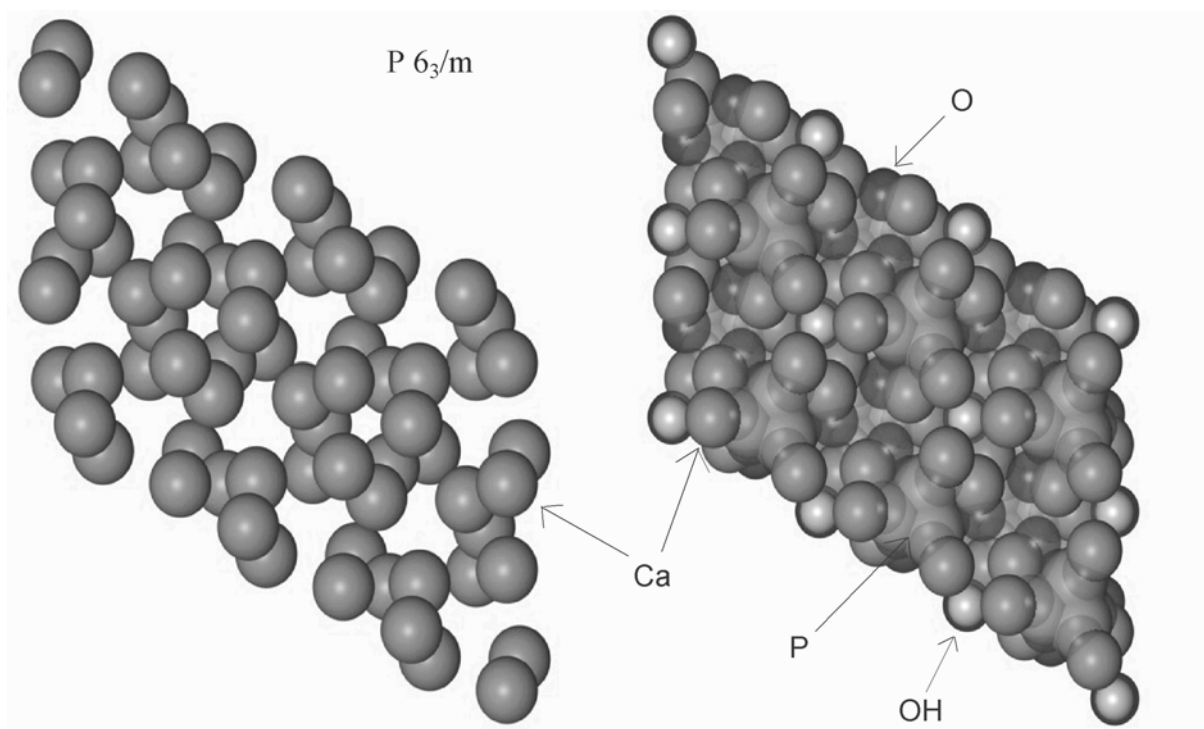


Figure 6: Explored initial HAP structure in the another representation (groups of symmetry are:  $P6_3/m$ ). Left only Ca-atoms presented.

As it follows from our direct *ab initio* quantum-chemical simulation and computer modeling the HAP actually form the channel-like structure for H-OH-channel

and proton can to move along this channel. We consider only first simple case of hexagonal symmetry group phase of HAP and obtain the results, which are confirmed with known experimental data and proposed models by another authors [1 –4, 15, 16, 18].

The size of calculated HAP nanoparticles are comparable with one of the experimentally obtained HAP nanoparticles powder size – it is on the order of ~ 10 nm.

The estimated value of surface charge follows from our HAP-nano-structure model is on the order ~ 0.1 C/m<sup>2</sup> , that correspond to experimental data range [1-4].

The main calculated HAP structures are the hexagonal symmetry. It is known that HAP has also another structure symmetry type – monoclinic, and has the phase transition between these two structures. Our further studies will develop the model including more details concerning monoclinic phase and stoichiometric change influences, too. At present, our model yet not consider the possible case of dehydration. However, we will elaborate it within the next model, since it is very important for more high temperature above ~ 600 grad Centigrade, as was discussed in [4].

## **5. CONCLUSION**

The main mechanism of HAP polarization and arising of surface charges is the proton transfer along H-OH... chains, as it follows from our direct *ab initio* simulation of HAP structure for the hexagonal symmetry group.

As results, were obtained detailed quantum-chemical computational structural models and calculated parameters of HAP nanoparticles for different symmetry groups. These results were obtained by using and adaptation of

HyperChem, Crystals, Gaussian-98 and by several special elaborated software.

The calculated structural HAP properties and peculiarities allow us to understand (to clarify) the mechanism of charge (proton) transport (transfer) and surface charging of HAP nanoparticles. The estimated values of surface charge is  $\sim 0.1 \text{ C/m}^2$  which is corresponded to known experimental data. These charges create the electric field up  $10^5 \dots 10^7 \text{ V/m}$  in the medium, which is influencing on the living cells motion and adhesion (immobilization) on the HAP nanoparticles and nanoceramics (PERCERAMICS) surface.

## ACKNOWLEDGEMENT

This work was supported by PERCERAMICS grant (No. NMP3-CT-2003-04937) from FP6 of EC.

## REFERENCES

1. N. Hitmi, D. Chatain, C. LaCabanne, J. Dugas, J.C.Trombe, C. Rey, G. Montel (1980): SC study of dipoles reorientations in hydroxyapatites. *Solid State Communications*, 33, 1003-1004.
2. N. Hitmi, C. LaCabanne, R.A. Young (1986): OH<sup>-</sup> dipole reorientability in hydroxyapatites: effect of tunnel size. *J. Phys. Chem. Solids*, 47, No.6, 533-546.
3. S. Nakamura, H. Takeda, K. Yamashita (2002): Proton transport polarization and depolarization of hydroxyapatite. *J. Appl. Phys.*, 89, No.10, 5386-5392.

4. M. Ueshima, S. Nakamura, K. Yamashita (2002): Huge, Millicoulomb Charge Storage in Ceramic Hydroxyapatite by Bimodal Electric Polarization. *Advanced Materials*, 14, No 8, 591- 595.
5. M.E. Lines, A.M. Glass (1977): *Principles and Applications of Ferroelectrics and Related Materials*.- Clarendon Press, Oxford.
6. H.R. Leuchtag, V.S. Bystrov (1999): Theoretical models of conformational transitions and ion conduction in voltage-dependent ion channels: Bioferroelectricity and superionic conduction. *FERROELECTRICS - 1999*. Vol. 220, No. 3-4. 157-204. (Special issue on "Ferroelectric and related models in biological systems.- Guest Editors: H. Richard Leuchtag and Vladimir S. Bystrov).
7. H.R. Leuchtag, V.S. Bystrov (2001): BioFerroelectricity. FERROELECTRIC AND RELATED MODELS IN BIOLOGICAL SYSTEMS. //Ferroelectricity Newsletter. A quarterly update on what's happening in the field of ferroelectricity. Vol. 9, No. 2, 7-8.  
<http://www.sp.nps.navy.mil/projects/ferro/vol9no2.pdf>
8. J.W. Goddby, R. Blinc, N.A. Clark, S.T. Lagerwall, M.A. Osipov, S.A. Pikin, T. Sakurai, K. Yoshino, B. Zeks (1991): *Ferroelectric Liquid Crystals: Principles, Properties and Applications*. – Gordon and Breach, Philadelphia.
9. J.M Hughes, M. Cameron, K.D. Crowley (1989): *American Mineralogist*, Vol. 74, 870-876. <ftp://ftp.geo.arizona.edu/pub/xtal/data/AMCfiles/01209.amc>
10. <http://www.xtl.ox.ac.uk/crystals.html>
11. <http://www.gaussian.com>
12. A. Bennis, F. Miskane, N. Hitmi, M.Vignoles, M. Heugherbaert, A. Lamure, C. LaCabanne (1992): Influence of defects and substitutions on polarization phenomena of bioelectrets. *IEEE Transactions on Electrical Insulation*, Vol. 27, No 4., 826.

13. S. Nakamura, T. Kobayashi, K. Yamashita (2002): Extended bioactivity in the proximity of hydroxyapatite ceramic surfaces induced by polarization charges, *J. Biomed. Mater. Res.*, 593-599.
14. T. Kobayashi, S. Nakamura, K. Yamashita (2001): Enhanced osteobonding by negative surface charges of electrically polarized hydroxyapatite. *J. Biomed. Mater. Res.*, 477-484.
15. N. Hitmi, E. Lamure-Plaino, A. Lamure, C. LaCabanne, R.A. Young (1986): Reorientable electric dipoles and cooperative phenomena in human tooth enamel. *Calcified Tissue International*, 38, 252-261.
16. G.C. Maiti, F. Freund (1981): Influence of fluorine substitution on the proton conductivity of hydroxyapatite. *J. Chem. Soc.*, 949-955.
17. M. Ueshima, S. Nakamura, M. Ohgaki, K. Yamashita (2002): Electrovectorial effect of polarized hydroxyapatite on quasi-epitaxial growth at nano-interfaces. *Solid State Ionics*, 151, 29-34.
18. K. Yamashita, K. Kitagaki, T. Umegaki (1995): Thermal instability and proton conductivity of ceramic hydroxyapatite at high temperatures. *J. Am. Ceram. Soc.*, 78(5), 1191-1197.
19. A.-V. Rousselle, D. Heymann (2002): Osteoclastic acidification pathways during bone resorption. *Bone*, 30, No. 4, 533-540.
20. L.L. Hench, R.J. Splinter, W.C. Allen, T.K. Greenlee (1971): Bonding mechanisms at the interface of ceramic prosthetic materials. *J. Biomed. Mater. Res. Symp.*, 2, 117-141.
21. M. Krukowski, R.A. Shiverly, P. Osdoby, B.L. Eppley (1990): Stimulation of craniofacial and intramedullary bone formation by negatively charged beads. *J. Oral Maxillofac. Surg.*, 48, 468-475.
22. M. Krukowski, D.J. Simmons, A. Summerfield, P. Osdoby (1988): *J. Bone Min. Res.*, 3, 165-171.

23. M. Ueshima, S.Tanaka, S. Nakamura, K. Yamashita (2002): *J. Biomed. Mater. Res.* 60, 578.
24. V.S. Bystrov, A.V. Saprionova, T.R. Tazieva, M.E. Green (2001). Non-linear dynamics of proton transfer in hydrogen-bonded systems.// *Physics of Vibrations*, 9, No. 3, 168-172.
25. V. Bystrov, M. Green, A. Saprionova, G. Ovtchinnikova, T. Tazieva, A. Soloshenko, B. Zapol (2002): Hydrogen bonds and Proton transfer in Ferroelectrics and related materials (molecular chains, proteins, DNA): Ab Initio GAUSSIAN-98 calculations and soliton models. In: *Proc. of the 13th IEEE ISAF from International Joint Conference on the Applications of Ferroelectrics 2002 (IFFF-2002)*. – May 28 – June 1, 2002. – Nara, Japan. – pp. 41-44.
26. A. Saprionova, V. S. Bystrov, M. E. Green (2003): Water, Proton Transfer and Hydrogen Bonding in Ion Channel Gating. *Frontiers of Biosciences*, September 1, 2003, vol.8, 1356-1370.  
<http://www.bioscience.org/current/vol8.htm>
27. <http://www.impb.ru> , [www.jcbi.ru](http://www.jcbi.ru) , [www.jscs.ru](http://www.jscs.ru)  
[http://www.impb.ru/index.php?id=div/opit/nano\\_res](http://www.impb.ru/index.php?id=div/opit/nano_res)